C.P. No. 797

C.P. No. 797

MINISTRY OF AVIATION

AERONAUTICAL RESEARCH COUNCIL

CURRENT PAPERS

The Steady Flow of a Viscous Fluid past a Circular Cylinder

By

S.C.R. Dennis (University of Sheffield)

and

M. Shimshoni (Weizmann Institute, Rehovot, Israel)

LONDON: HER MAJESTY'S STATIONERY OFFICE

1965

Price 8s. 6d. net

C.P. No. 797

August, 1964

THE STEADY FLOW OF A VISCOUS FLUID PAST A CIRCULAR CYLINDER

-by-

S. C. R. Dennis (University of Sheffield)

and

M. Shimshoni (Weizmann Institute, Rehovot, Israel)

SUMMARY

Using numerical methods described in a previous paper (Dennis and Dunwoody, 1964), the steady motion of a viscous, incompressible, fluid past a fixed circular cylinder is investigated over the complete range of Reynolds numbers. In particular, the limiting solution as the Reynolds number R becomes large is considered.

The calculated drag coefficient is found to agree reasonably well with experimental measurements for low Reynolds numbers but starts to become higher for values of R greater than about 30. For large Reynolds numbers the theoretical estimate of the pressure drag tends to become constant while the frictional drag decreases proportionately to the square root of the Reynolds number. This tendency of the pressure drag greatly to exceed the frictional drag for large values of R has already been noted in experimental work.

Secondly, with regard to the detailed flow patterns, the calculations show that for Reynolds numbers below R = 5.6 a non-separated flow takes place past the cylinder. The value R = 5.6 at which the standing vortex pair first appear behind the cylinder is in good agreement with the experimental estimates of Homann (1936) and Taneda (1956). As the Reynolds number increases the length of the vortex pair, measured downstream from the rear generator of the cylinder, increases and at R = 30 it exceeds the length of the diameter of the cylinder. At R =40 , however, the length of the vortices has decreased according to the present solution; and it continues to decrease as the Reynolds number is further increased. It is pointed out, however, that the description of this feature of the flow, viz. the behaviour of the vortices as R becomes large, is somewhat tentative owing to the necessity of limiting the size of the calculations.

At very low Reynolds numbers the calculated solutions agree with the solution of Oseen's linearised equations. Some aspects of the Oseen linearised solution are discussed in detail in the present paper since it is found that they do not agree with the previously published results of Tomotika and Aoi (1950).

Replaces A.R.C.26 104.

INTRODUCTION

The governing equations applicable to the present investigation and the method of numerical solution by which they are solved are essentially as described by Dennis and Dunwoody (1964) in a previous paper concerned with steady flow past a flat plate. For steady two-dimensional flow past a circular cylinder the appropriate coordinates are polar coordinates (r,θ). The dependent variables are the stream function $\psi(r,\theta)$ and the scalar vorticity $\zeta(r,\theta)$. The first is defined in terms of the radial and transverse velocity components (v_r, v_θ) by the equations

$$v_r = \frac{1}{r}\frac{\partial \psi}{\partial \theta}, \qquad v_\theta = -\frac{\partial \psi}{\partial r}. \tag{1}$$

Equations (1) satisfy the equation of continuity of the fluid, which is assumed to be incompressible. The vorticity is expressed in terms of the velocity components by the equation

$$\zeta = \frac{\partial v_\theta}{\partial r} + \frac{v_\theta}{r} - \frac{1}{r}\frac{\partial v_r}{\partial \theta}. \tag{2}$$

The governing equation for ζ is obtained by eliminating the pressure from the Navier-Stokes equations of motion. This gives

$$\nu\left(\frac{\partial^2 \zeta}{\partial r^2} + \frac{1}{r}\frac{\partial \zeta}{\partial r} + \frac{1}{r^2}\frac{\partial^2 \zeta}{\partial \theta^2}\right) = \frac{1}{r}\left(\frac{\partial \psi}{\partial \theta}\frac{\partial \zeta}{\partial r} - \frac{\partial \psi}{\partial r}\frac{\partial \zeta}{\partial \theta}\right), \tag{3}$$

where ν is the coefficient of kinematical viscosity.

Equations (1), (2) and (3) must be solved in conjunction with the no-slip condition $v_r = v_\theta = 0$ at the surface of the cylinder, $r = a$. If also the flow at large distances from the cylinder is a uniform stream with velocity U parallel to the positive direction of the x-axis, the appropriate conditions are that

$$v_r \to U\cos\theta, \qquad v_\theta \to -U\sin\theta, \qquad \text{as } r \to \infty. \tag{4}$$

Previous theoretical results for the steady motion of a viscous fluid past a circular cylinder may be roughly divided into two categories. Firstly, there are solutions of Oseen's linearised equations, valid at low Reynolds numbers. An approximate solution of Oseen's equations was first given by Lamb (1911) and subsequently extended by both Bairstow, Cave and Lang (1923) and Tomotika and Aoi (1950). This extension has been criticized by Proudman and Pearson (1957). The objection is that Lamb's solution is already correct to the order of approximation necessarily inherent in approximating to the true equations of motion by Oseen's equations, and that nothing is added by obtaining higher order approximations to the solution of the latter. Kaplun (1957) has given what is considered to be the valid correction to Lamb's solution.

A further point about Tomotika and Aoi's solution is that it purports to show that a separated flow, viz. one in which a pair of standing eddies is formed behind the cylinder, exists for all values of the Reynolds number, however small. This is in direct conflict with experiment. It is known experimentally that, below a certain critical Reynolds number, no separation takes place. The actual critical value is variously estimated at 3.2 by Nisi and Porter (1923), 6 by Homann (1936) and 5 by Taneda (1956). Since these values of the Reynolds number are beyond the range of validity of Oseen theory, no theoretical confirmation of this result has yet been obtained.

Secondly, there are the approximate numerical solutions of the full equations of motion, i.e. the solution of Thom (1929) at R = 10, Thom (1933) at R = 20, Kawaguti (1953) and Apelt (1961), both at R = 40 and finally Allen and Southwell (1955) at R = 0, 1, 10, 100 and 1000. Allen and Southwell cover the largest range of Reynolds numbers but their results have recently been

criticized by Kawaguti (1959), whose main objection is to the detailed flow patterns round the cylinder given by these results. Kawaguti suggests that all the evidence of previous investigations of the problem indicates that the standing vortex pair behind the cylinder should elongate with increasing Reynolds number and that Allen and Southwell's flow patterns at R = 100 and 1000 are not in accordance with this. None the less, Allen and Southwell's results are the only moderately high Reynolds number results that have so far been attempted.

In the present paper, results are obtained for the complete range of Reynolds numbers from 0.01 up to indefinitely large values. At the lower end of the scale, where the numerical solutions are believed to be extremely accurate, the object is to compare the results of the various theories and determine accurately the Reynolds number at which separation starts to occur. At intermediate and higher Reynolds number an attempt is made to correlate existing numerical results and determine the general features of the flow as R becomes large.

To reduce the problem to a form comparable with that solved in the case of the flat plate, we make the transformation

$$r = ae^{\xi}, \quad \theta = \eta \tag{5}$$

and introduce the dimensionless quantities defined by the equations

$$\psi = Ua\psi', \quad \zeta = \frac{U}{a}\zeta', \quad R = \frac{2aU}{\nu}, \tag{6}$$

where a is the radius of the cylinder. Suppressing primes, equation (3) becomes

$$\nabla^2\zeta = \frac{R}{2}\left(\frac{\partial\psi}{\partial\eta}\frac{\partial\zeta}{\partial\xi} - \frac{\partial\psi}{\partial\xi}\frac{\partial\zeta}{\partial\eta}\right) \tag{7}$$

while (1) and (2) together give

$$\nabla^2\psi + e^{2\xi}\zeta = 0, \tag{8}$$

where $\nabla^2 = \partial^2/\partial\xi^2 + \partial^2/\partial\eta^2$.

The boundary conditions $v_r = v_\theta = 0$ on the cylinder give rise to the conditions

$$\psi = \frac{\partial\psi}{\partial\xi} = 0, \quad \text{when } \xi = 0 \tag{9a}$$

while the free stream conditions (4) become

$$\frac{1}{e^{\xi}\sin\eta}\frac{\partial\psi}{\partial\xi} \to 1, \qquad \frac{1}{e^{\xi}\sin\eta}\frac{\partial\psi}{\partial\eta} \to 1, \quad \text{as } \xi \to \infty. \tag{9b}$$

By the symmetry of the motion about the x-axis we also obtain

$$\psi = \zeta = 0 \quad \text{when } \eta = 0, \pi. \tag{9c}$$

It may now be observed that the mathematical problem involved in solving (7) and (8) is almost identical with that described in the paper by Dennis and Dunwoody in the case of a flat plate. This paper will subsequently be referred to as I. The method of numerical analysis used is identical and only those features especially relating to the case of the circular cylinder need be mentioned.

DETAILS OF THE SOLUTION FOR A CIRCULAR CYLINDER

Equations (7) and (8) are reduced to ordinary differential equations by the same substitutions as in I, viz.

$$\psi(\xi,\eta) = \sum_{n=1}^{\infty} f_n(\xi) \sin n\eta \tag{10}$$

and

$$\zeta(\xi,\eta) = e^{F(\xi,\eta)} \sum_{n=1}^{\infty} g_n(\xi)\sin n\eta. \tag{11}$$

Equation (8) is reduced to the set of equations

$$f_n'' - n^2 f_n + r_n(\xi) = 0, \qquad (n = 1,2,3,\ldots\ldots) \tag{12}$$

with

$$r_n(\xi) = \sum_{p=1}^{\infty}{}' g_p(\mathcal{J}_{n-p} - \mathcal{J}_{n+p})e^{2\xi} \tag{13}$$

and, as before,

$$\mathcal{J}_n(\xi) = \frac{1}{\pi}\int_0^{\pi} e^{F(\xi,\eta)}\cos n\eta \, d\eta. \tag{14}$$

The only essential change is therefore in the definition of $r_n(\xi)$, which is less complicated.

The boundary conditions (9a) give the same initial conditions for the $f_n(\xi)$, i.e.

$$f_n(0) = f_n'(0) = 0, \quad (n = 1,2,3,.....). \tag{15}$$

At large distances, (9b) lead to the conditions

$$e^{-\xi}f_1(\xi) \to 1, \qquad e^{-\xi}f_n(\xi) \to 0 \quad (n \neq 1) \quad , \tag{16}$$

so there is a slight difference in a numerical factor from the case of the flat plate.

If we follow the analysis used in I to determine the form of ψ at large distances, it is readily deduced that, as $\xi \to \infty$,

$$\psi(\xi,\eta) \sim e^{\xi}\sin\eta + K(1 - \frac{\eta}{\pi}) \tag{17}$$

The value of the constant K is obtained, as in I, from the theorem of Goldstein (1929). This gives

$$K = -\frac{D}{2\rho U^2 a} = -\tfrac{1}{2}C_D \quad , \tag{18}$$

where C_D is the drag coefficient.

The drag D is found by evaluating the integral (31) in I round the contour of the cylinder. This yields

$$D = -\int_0^{2\pi} (pa\cos\eta + \rho\nu U\zeta\sin\eta)d\eta \quad , \tag{19}$$

where p and ρ are the pressure and density and ζ is non-dimensional. The part of this integral depending on the viscosity gives the frictional drag D_f. By symmetry

$$D_f = -2\rho\nu U \int_0^\pi \zeta_0 \sin\eta \, d\eta \, , \tag{20}$$

where ζ_0 is the value at $\xi = 0$. Now, as in I, the function $F(\xi,\eta)$ in (11) is chosen to satisfy the equation

$$\frac{\partial F}{\partial \xi} = \frac{1}{4}R\frac{\partial \psi}{\partial \eta} \tag{21}$$

and also the condition

$$F(0,\eta) = 0.$$

Hence substituting for ζ_0 in the above integral from (11) we obtain

$$D_f = -\pi\rho\nu U g_1(0)$$

and the corresponding dimensionless drag coefficient is

$$C_f = \frac{D_f}{\rho U^2 a} = -\frac{2\pi}{R} g_1(0). \tag{22}$$

The term in (19) involving the pressure likewise gives the pressure drag D_p, i.e.

$$D_p = -2a \int_0^\pi p_0 \cos\eta \, d\eta$$

$$= 2a \int_0^\pi \left(\frac{\partial p}{\partial \eta}\right)_0 \sin\eta \, d\eta,$$

on integrating by parts, where the suffix zero again refers to $\xi = 0$. If the equations of motion are expressed in terms of ξ and η it is easy to show that

$$\left(\frac{\partial p}{\partial \eta}\right)_0 = \frac{\rho\nu U}{a}\left(\frac{\partial \zeta}{\partial \xi}\right)_0.$$

Substituting in the integral and differentiating (11) with regard to ξ, using the fact that $(\partial F/\partial \xi)_0 = 0$ from (21), we obtain

$$D_p = \pi\rho\nu U g_1'(0)$$

and hence

$$C_p = \frac{D_p}{\rho U^2 a} = \frac{2\pi}{R} g_1'(0). \qquad (23)$$

The ratio of the pressure drag to the frictional drag is therefore $-g_1'(0)/g_1(0)$. It is subsequently found that this ratio tends to unity as R is indefinitely decreased, in agreement with Oseen theory. When R becomes large the ratio increases as $R^{\frac{1}{2}}$.

The governing equation (7) for the vorticity is identical with the corresponding equation for the case of the flat plate. Using the substitution (11), the method of treating it is identically that described in I, viz. it is reduced to a set of equations

$$g_n'' - n^2 g_n + \sum_{p=1}^{\infty} k_{n,p} g_p = 0, \qquad (n = 1,2,3,.....), \qquad (24)$$

where $k_{n,p}(\xi)$ and all the associated functions are exactly as defined in I. Numerical solutions are obtained precisely as before; they are finally expressed in the form

$$g_n(\xi) = C_1 G_n(\xi), \qquad (n = 1,2,3,.....) \qquad (25)$$

with

$$G_1(0) = 1. \qquad (26)$$

As for the flat plate, the solutions (25) are supposed to have been chosen to satisfy a condition which ensures that $\psi(\xi,\eta)$ tends to the correct form (17) for large ξ. The method of satisfying the condition is as described in I, although the condition itself is modified by a numerical factor on account of the different numerical factor in the first of (16). A first integral of (12) is

$$f_n' + nf_n + e^{n\xi} \int_0^{\xi} e^{-nt} r_n(t)dt = B_n e^{n\xi},$$

where B_n are all zero by (15). Dividing each side by $e^{n\xi}$, letting $\xi \to \infty$ and using (16), then

$$\left.\begin{aligned} \int_0^\infty e^{-n\xi} r_n(\xi)\,d\xi &= -2 \quad (n = 1) \\ &= 0 \quad (n \neq 1). \end{aligned}\right\} \tag{27}$$

Finally, in terms of the solutions (25), the total drag coefficient is given by

$$C_D = -\frac{2\pi C}{R}\{1 - G_1'(0)\}\,, \tag{28}$$

the two separate terms corresponding to the frictional and pressure drags respectively.

CALCULATIONS AT LOW REYNOLDS NUMBERS

In this section the results of calculations for low values of the Reynolds number are compared with Oseen theory and modifications to this theory.

In effect, the Oseen linearised solution may be obtained by substituting the outer boundary conditions (9b) for ψ into (7), which becomes

$$\nabla^2 \zeta = \frac{R}{2} e^{\xi} \left(\cos\eta \frac{\partial \zeta}{\partial \xi} - \sin\eta \frac{\partial \zeta}{\partial \eta} \right).$$

Substituting the expression (11) for ζ, and making

$$F(\xi, \eta) = \frac{1}{4} R e^{\xi} \cos\eta\,, \tag{29}$$

equations (24) for the functions $g_n(\xi)$ become

$$g_n'' - (n^2 + \frac{d^2}{16} e^{2\xi}) g_n = 0.$$

Fundamental solutions which vanish for large ξ are

$$g_n(\xi) = K_n(\beta),$$

where K_n is the modified Bessel function of the second kind and

$$\beta = \frac{1}{4} R e^{\xi} \quad .$$

We may therefore take the functions $G_n(\xi)$ in (25) as

$$G_n(\xi) = A_n \frac{K_n(\beta)}{K_n(R/4)} \quad , \tag{30}$$

where $A_1 = 1$ in order to satisfy (26).

This solution is valid for large ξ and is, with minor changes, the solution at large distances discussed in I. In Oseen theory, however, it is assumed to hold for all ξ. To find the constants A_n $(n = 2,3,4,....)$ we substitute in the second of the conditions (27), noting that the function $\mathcal{J}_n(\xi)$ is now the modified Bessel function of the first kind with argument β, viz.

$$I_n(\beta) = \frac{1}{\pi} \int_0^{\pi} e^{\beta \cos\eta} \cos n\eta \, d\eta \quad .$$

This gives the set of simultaneous equations

$$\sum_{p=1}^{\infty} \lambda_{n,p} A_p = 0, \quad (n = 2,3,4,....) \tag{31}$$

where

$$\lambda_{n,p} = \frac{1}{K_p(R/4)} \int_0^{\infty} e^{(2-n)\xi} \{ I_{n-p}(\beta) - I_{n+p}(\beta) \} K_p(\beta) \, d\xi. \tag{32}$$

Writing $\mu_{n,p} = \lambda_{n,p} K_p(R/4)$

then $\mu_{n,p}$ denotes the integral in (32). This integral may be evaluated by expressing the integrand as a function of β alone and making use of the result

$$\frac{d}{d\beta} \left\{ \beta^p [I_q(\beta) K_r(\beta) + I_{q+1}(\beta) K_{r+1}(\beta)] \right\}$$

$$= \beta^{p-1} \left\{ (p+q+r) I_q(\beta) K_r(\beta) + (p-q-r-2) I_{q+1}(\beta) K_{r+1}(\beta) \right\} ,$$

where p, q and r are any integers. This result is given by Watson (1944) for the cylinder functions but it is equally valid for the modified Bessel functions. By suitable choice of p, q and r it follows that

$$2(n-1)\mu_{n,p} = I_{n-p-1}K_{p-1}+I_{n-p}K_{p} - I_{n+p-1}K_{p+1}-I_{n+p}K_{p}, \tag{33}$$

provided $n \neq 1$, while

$$\mu_{1,p} = \frac{4}{R}\sum_{q=1}^{p}(I_{q-1}K_{q-1} + I_{q}K_{q}). \tag{34}$$

In these formulae the arguments of all the Bessel Functions are R/4.

Since $A_1 = 1$, the remainder of the A_n can be found by solving equations (31). Without going into detail it may be shown, by expanding the Bessel functions in (33) in terms of R, that as $R \to 0$ the first order solution of (31) is

$$A_{n+1} = O(R^n \log R), \quad (n = 1,2,3,.....). \tag{35}$$

Now the equation determining the constant C_1 which occurs in (25) is, from the first of (27)

$$C_1 \sum_{p=1}^{\infty} \lambda_{1,p}A_p = -2.$$

In obtaining a first approximation to C_1 we can, by (35), omit all the A_n except A_1, which is unity, from this equation. Using (34), this gives

$$C_1 \approx -\frac{RK_1}{2(I_oK_o+I_1K_1)}, \tag{36}$$

where the arguments of the Bessel functions are again $\frac{1}{4}R$.

The formula (28) for the drag coefficient does not apply to the Oseen solution. This formula depends upon the satisfaction of the conditions $F = \partial F/\partial\xi = 0$, when $\xi = 0$. In the numerical solutions of the full equation

(7) the function $F(\xi,\eta)$ is chosen to satisfy these conditions but, by (29), the Oseen solution does not. To obtain the drag we must return to the basic formulae and substitute the details of the Oseen theory. Substituting for ζ in (20) it is readily verified that we obtain a frictional drag coefficient

$$C_f = -\frac{16\pi C_1}{R^2} \sum_{n=1}^{\infty} n A_n I_n K_n \quad . \tag{37}$$

Similarly, the basic formula for the pressure drag is

$$D_p = 2\rho\nu U \int_0^{\pi} \left(\frac{\partial\zeta}{\partial\xi}\right)_0 \sin\eta \, d\eta$$

and if we substitute for $(\partial\zeta/\partial\xi)_0$ we obtain, after some reductions of Bessel functions,

$$C_p = C_f - \tfrac{1}{2}\pi C_1 \sum_{n=1}^{\infty} (I_{n-1}K_{n-1} - I_{n+1}K_{n+1})A_n \quad . \tag{38}$$

In both these formulae the arguments of the Bessel functions are $R/4$. Alternatively a formula for the total drag can be obtained from (18) by determining a value for K. It is found (cf Dennis and Dunwoody) that this gives

$$C_D = -\frac{16\pi C_1}{R^2} \sum_{n=1}^{\infty} n A_n \quad . \tag{39}$$

For low Reynolds numbers the terms arising from the summation in (38) are of higher order than the leading term in C_f. Hence for small enough R, $C_f \asymp C_p$. Tomotika and Aoi claim that this result holds exactly for any Reynolds number, according to Oseen theory. We cannot find such an exact relationship; moreover, the result (39) for the total drag is not exactly consistent with that obtained from (37) and (38). If, however, we take the value of C_1 given

by (36) and expand all the Bessel functions in terms of R, retaining only first order terms, we obtain Lamb's original result

$$C_D = \frac{8\pi}{R(\frac{1}{2}-\gamma-\log R/8)} \tag{40}$$

consistently from either (39) or (37) and (38). This is in agreement with the general observations made by Proudman and Pearson, viz. that Lamb's formula is already correct to the order of accuracy involved in approximating to the exact governing equations by Oseen theory and that there is no virtue in improving it. On this basis the refinements of Oseen theory given by Bairstow, Cave and Lang and by Tomotika and Aoi are hardly valid. Kaplun has given a second approximation to Lamb's solution which is based on the exact Navier-Stokes equations. This is obtained by matching a solution of Oseen's equations far enough from the cylinder with an inner solution based on Stokes' theory. If

$$\epsilon = (\tfrac{1}{2}-\gamma-\log R/8)^{-1} ,$$

Kaplun suggests that the correct development of (40) according to the exact equations should be

$$C_D = \frac{8\pi}{R}\,\epsilon\left(1 + \sum_{n=2}^{\infty} d_n \epsilon^n\right) \tag{41}$$

and calculates the value $d_2 = -0.87$.

Another aspect of Tomotika and Aoi's solution of Oseen's equations is the description of the detailed flow patterns it gives for very low Reynolds numbers. According to their calculations a separated flow, with a pair of standing eddies behind the cylinder, exists for all small values of R, no matter how small. This contradicts experimental evidence; and one might suppose that some small enough value of R could be found below which Oseen theory predicts

a non-separated flow, in accordance with the experimental results.

To consider the question of the formation of the standing eddies, the equation of the separated streamline is $\psi = 0$ and the angular coordinate of the point of separation is found by putting $\xi = 0$ in equation (10) for ψ. In view of (15) we may replace $f_n(0)$ by $f_n''(0)$ and moreover divide out the factor $\sin\eta$, whose vanishing gives the known streamlines $\eta = 0$ and $\eta = \pi$. The result is the equation

$$f_1''(0) + 2f_2''(0)\cos\eta + f_3''(0)(3 - 4\sin^2\eta) + \ldots = 0, \tag{42}$$

which is valid for any solution in the form (10). In the case of the Oseen solution obtained in this section, the first order solution for $f_n''(0)$ is obtained directly from the differential equations (12) by substituting the first order solution for $r_n(0)$. The latter is easily obtained once the first order solution for the constants A_n has been obtained and, without going into detail, it is found that for $n > 0$

$$f_{n+1}''(0)/f_1''(0) = O(R^n \log R)$$

at least. Also $f_1''(0) > 0$ and $f_2''(0) < 0$, as $R \to 0$.

Hence for small enough R, according to our solution of Oseen's equations, the first two terms of (42) dominate and approximately

$$\cos\eta = -f_1''(0)/2f_2''(0) \gg 1$$

and no separation takes place. If, as R is increased, a stage is reached at which separation starts to occur, the angle of separation at which it first occurs will be given by $\cos\eta = 1$, i.e. the fluid starts to separate from the rear generator of the cylinder. The critical value of R will then be that value which makes

$$S = \sum_{n=1}^{\infty} n f_n''(0) = 0 \tag{43}$$

In the present paper solutions of the exact Oseen equations have been obtained in two ways, firstly by obtaining accurate numerical solutions of the equations (31), and secondly by solving the complete Oseen problem using numerical techniques previously described. In the latter case it is easily arranged that the same computer programme which solves the general f_n and g_n-equations (12) and (24) shall include Oseen theory as a special case. By comparing the two solutions we then obtain some check on the efficiency and accuracy of the numerical methods. As this check was being carried out, the sum S was evaluated. It was found that as $R \to 0$

$$S \sim f_1''(0) > 0,$$

in accordance with the above, and that S decreases as R increases, becoming zero at about R = 3. The comparison between the two solutions was uniformly good, e.g. the results at R = 3 are typical. Here it was found from the analytical solution that $C_1 = -2.056$, correct to three decimals, while

$$f_1''(0) = 1.584, \quad f_2''(0) = -0.899, \quad f_3''(0) = 0.065, \quad f_4''(0) = 0.005.$$

The corresponding figures from the numerical solution of Oseen's equations were $C_1 = -2.059$ with

$$f_1''(0) = 1.587, \quad f_2''(0) = -0.901, \quad f_3''(0) = 0.065, \quad f_4''(0) = 0.005.$$

In both solutions $f_5''(0) = 0.0002$, i.e. the convergence appears quite good.

These accurate solutions of Oseen's equations are, of course, subject to Proudman and Pearson's criticisms. They do, however, predict the existence of a critical Reynolds number, contrary to Tomotika and Aoi's account of the theory. The value is about half of the value (R=6) that we obtain from the numerical solutions of the full Navier-Stokes equations given in table 3 in the following section.

In table 1, values of the drag coefficient calculated by present methods from the full Navier-Stokes equations are compared with values obtained from Lamb's formula (40) and from Kaplun's result (41) (including only the term in d_2). It might, perhaps, have been expected that slightly better agreement with Kaplun's results would have been obtained at the very low Reynolds numbers, since our results are thought to be reasonably accurate here.

CALCULATED RESULTS

Calculated frictional and pressure drag coefficients, together with the total drag coefficient C_D , are given in table 2. In figure 1, C_D is compared with experimental measurements and with previous numerical integrations of the exact Navier-Stokes equations. The experimental curve (based on measurements carried out at the National Physical Laboratory and at Göttingen) has been taken directly from Goldstein (1938) since this curve seems to cover the largest Reynolds number range. At the lower Reynolds number end of the range, comparison is also made with the recent experimental results of Tritton (1959) in figure 2. Tritton's results for $R > 50$ are a little lower than the experimental values in figure 1, although the latter are largely confirmed by the experiments of Wieselsberger (1921). It will be noticed that the present theoretical results become increasingly higher than the observed values as R increases beyond about 30. As R becomes large the theoretical pressure drag becomes constant while the frictional drag tends to zero; this tendency has been

observed in experimental work [Blasius (1913), Thom (1930)].

The theoretical result for large R can be demonstrated by obtaining a limiting solution of equations (24) as $R \to \infty$ in the manner previously described by Dennis and Dunwoody. It was there shown that by making the transformation $\xi = \delta z$, so that (24) become

$$\frac{d^2 g_n}{dz^2} - \delta^2 n^2 g_n + \delta^2 \sum_{p=1}^{\infty} k_{n,p} g_p = 0 , \qquad (45)$$

the quantity δ could be chosen in such a way that $\delta \to 0$ as $R \to \infty$ and

$$\delta^2 k_{n,p} \sim K_{n,p}(z) ,$$

where the $K_{n,p}$ are independent of R. Solutions of (45) can then be found, as $\delta \to 0$, as functions of z alone. The necessary choice of δ is to make it satisfy the relation

$$\delta^3 R C_1 = c$$

and it is then found that in order to satisfy the conditions of type (27) we must have

$$C_1 = a\delta^{-1} .$$

Here a and c are numerical constants; the constant c may be assigned and the value of a then depends upon the solutions computed from (45).

In the present case the value $c = -21.47$ was taken. From the computed solutions of (45) it was found that

$$a = -2.30; \quad (dg_1/dz)_0 = -0.838 .$$

Hence

$$\delta = 3.05R^{-\frac{1}{2}}, \quad C_1 = -0.753R^{\frac{1}{2}} .$$

The limit of the frictional drag coefficient is therefore

$$c_f = 4.73R^{-\frac{1}{2}}$$

and the limit of the pressure drag coefficient is

$$C_p = \frac{2\pi C_1}{R\delta}\left(\frac{dg_1}{dz}\right)_o = 1.300 \quad .$$

Owing to limitations of computer storage space it was found necessary to restrict the calculations to five terms $g_n(\xi)$ of the series (11). Expressing these in the form (25), we may calculate an approximation to the vorticity distribution over the surface of the cylinder in the form

$$\zeta(0,\eta) = C_1 \sum_{n=1}^{5} G_n(0)\sin n\eta \quad . \tag{46}$$

Some sets of values of the $G_n(0)$ with the constant C_1 are shown for values of R up to 160 in table 3. Beyond R=160 these constants may not be very accurate, since their values may be affected by truncation of the series (11). However, the vorticity distribution is shown graphically for various Reynolds numbers in figure 3.

At the point of the surface where $\zeta=0$ (i.e. the local shearing stress vanishes), the fluid separates from the cylinder. The condition $\zeta = 0$ for separation is consistent with (42) since

$$f_n''(0) = -r_n(0) = -C_1 G_n(0).$$

From (43), the critical value of R is therefore the value which makes

$$S' = \sum_{n=1}^{\infty} nG_n(0) = 0 \quad .$$

On the basis of the values in table 3 we find that $S' = 0.121$ for R= 4

and $S' = -0.106$ for $R = 7$. A linear interpolation therefore gives the critical value as $R = 5.6$, which is in good agreement with the experimental estimates of Taneda and Homann.

One of the interesting features of the present problem is the question of the growth of the standing vortices behind the cylinder as the Reynolds number increases. In figures 4 to 10, streamlines are shown for the flow past the upper half of the cylinder for a range of Reynolds numbers from 4 to 80; the function tabulated is the dimensionless stream function ψ' defined by the first of equations (6). Denoting the length of the vortex pair by d (as shown in figure 5) it will be seen that d steadily increases up to $R = 30$. Its value of about one diameter at $R = 20$ is in good agreement with the estimate of Thom. At $R = 33.5$ (not shown) d is found to have about the same value as at $R = 30$ but thereafter it decreases, as indicated in figures 9 and 10. At $R = 160$ it is not more than 0.3a and for larger values of R it decreases still further. In this respect the present solutions for $R > 30$ are different from previously published results. At $R = 40$ Kawaguti finds d to be almost two diameters of the cylinder and Apelt gives 2.13 diameters, increasing to 2.3 diameters at $R = 44$. Allen and Southwell's results suggest that d decreases for higher Reynolds numbers, but hardly on the scale suggested by the present solutions.

Figure 11 shows graphically the various estimates, theoretical and experimental, of the ratio d/2a as a function of R. It must be noted that the theoretical results of Kawaguti and Apelt are in good agreement

with the experimental estimates of Taneda, who measured the length of the standing vortex pair up to R = 57.7. The significance of this is difficult to judge, however, since it is well known that within the range R = 30 to 50 the onset of the Karman vortex street is observed in the wake. The actual Reynolds number at which the street appears is variably estimated and seems to depend considerably upon external conditions, such as the ratio of the cylinder diameter to the experimental channel width. Since the Karman vortex street is not a steady state, it cannot be described by the present equations. It is therefore not easy to see what the relation between solutions of these equations and experimental observations should be with regard to the growth of the vortices in the critical region of R at which the street appears. The main objection to the present solutions with regard to their description of the behaviour of the vortices is that only a limited number (five) of terms have been used in calculating the stream function. Without further investigation, it is impossible to say what the effect of including further terms would be, so that our conclusions with regard to this phenomenon must to this extent be tentative*. It seems, however, rather coincidental that the tendency of d to decrease starts to occur in the neighbourhood of the critical Reynolds number at which the vortex street appears.

The only comment that could be made on Apelt and Kawaguti's numerical solutions is that, compared with the present solutions, the mesh lengths of the relaxation fields are a little coarse. Kawaguti works in terms of the variables

---

*The series for ψ certainly converges more slowly in the wake at larger distances from the cylinder than it does near the cylinder and this may affect the estimation of the length of the vortices. This point is under investigation.

$$X = a/r, \quad Y = 2\eta/\pi$$

and divides the range outside the cylinder ($X = 1$ to $X = 0$) into ten intervals. The row of mesh points next to the cylinder therefore corresponds to the value $\xi = 0.105$ and the spacing between mesh points in the ξ-coordinate increases with ξ. To obtain a reasonable solution at $R = 40$ we found it necessary to take a step $h = 0.025$ in the ξ-coordinate. For higher values of R (and also in the previous calculations of Dennis and Dunwoody for the flat plate) the step h was adjusted to be approximately proportional to $R^{-\frac{1}{2}}$. Apelt's mesh length for $R = 40$ is even coarser than Kawaguti's, corresponding to a step $h = \pi/20$ in the ξ-coordinate.

The vorticity distribution throughout the flow field is determined from (11). The form of this distribution near the cylinder is shown for some representative Reynolds numbers in figures 12-15 . As R increases the vorticity tends to become more and more concentrated into the region near the surface of the cylinder and in the laminar wake behind the cylinder. Even at very high Reynolds numbers it is found that the effect of the wake is important, leading to a resultant pressure drag on the cylinder. This may be seen as follows.

It was shown in I that as $\xi \to \infty$

$$r_n(\xi) \to nC = 2nK/\pi , \qquad (47)$$

where K is the constant (depending on R) which appears in (17). This limiting form is satisfied automatically by the numerical solutions on satisfying the initial conditions (15) and the conditions (27); and it is easily shown, using Oseen theory, that it corresponds to a

vorticity distribution concentrated into a wake near $\eta = 0$ as ξ becomes large. Near enough to $\eta = 0$, equation (11) may be written

$$\zeta(\xi,\eta) = \eta e^{F(\xi,\eta)} \sum_{n=1}^{\infty} n g_n(\xi) .$$

For any R and large enough ξ we have, from Oseen theory

$$g_n(\xi) \sim d_n K_n(\beta), \quad F(\xi,\eta) \sim \beta\cos\eta ,$$

where

$$\beta = \frac{1}{4} R e^{\xi}.$$

Since ξ is large

$$K_n(\beta) \sim \left(\frac{\pi}{2\beta}\right)^{\frac{1}{2}} e^{-\beta}$$

and hence

$$\zeta \sim e^{\beta(\cos\eta - 1)} \left(\frac{\pi}{2\beta}\right)^{\frac{1}{2}} \eta \sum_{n=1}^{\infty} n d_n . \tag{48}$$

The vorticity is therefore exponentially small everywhere except in the wake whose boundary is given by

$$\eta_1 = O(\beta^{-\frac{1}{2}}) \tag{49}$$

which ultimately coincides with $\eta = 0$. Also, by comparing the governing equation (8) with the transformed analogue (12), we have

$$r_n(\xi) = \frac{2e^{2\xi}}{\pi} \int_0^{\pi} \zeta \sin n\eta \, d\eta .$$

For large enough ξ we may replace the upper limit by η_1 and write

$$r_n(\xi) \sim \frac{2ne^{2\xi}}{\pi} \int_0^{\eta_1} \zeta\eta d\eta$$

and using (48) and (49) it is seen that this leads to the form (47).

The strength of the vorticity in the wake therefore depends directly on the constant C which, by (18), is directly proportional to the drag coefficient C_D. Thus the tendency of C_D to become constant as R becomes large is associated with an appreciable residual vorticity in the wake which persists for large R. It is in fact found from the numerical solutions as R becomes large that the vorticity (which becomes proportional to $R^{\frac{1}{2}}$ on the cylinder) falls very rapidly in the wake near the cylinder but then decays more slowly in the wake at larger distances.

The slower decay in the wake at larger distances does not, however, destroy the concept of the boundary layer thickness $\xi = \delta$ which has been used in computing solutions at higher Reynolds numbers. It has been explained in I that δ is a number used to replace the upper limit in the integral in (27) in estimating values of the constants associated with the solutions of (24). Although for large enough ξ the $r_n(\xi)$ must assume the form (47) and, as $R \to \infty$, C tends to an absolute constant, it has been pointed out in I that in practice we record the functions $R_n(\xi)$ defined by

$$r_n(\xi) = -C_1 R_n(\xi), \quad (n = 1,2,3,.....) .$$

In effect, therefore, the integral

$$\int_0^{\delta} e^{-n\xi} R_n(\xi) d\xi \tag{50}$$

is evaluated in (27). As $R \to \infty$, $C_1 = O(R^{\frac{1}{2}})$, so that near $\xi = 0$ the $R_n(\xi)$ are $O(1)$ and at $\xi = \delta$ they are $O(R^{-\frac{1}{2}})$. The value of δ is there-

adjusted so that the $O(R^{-\frac{1}{2}})$ contribution to (50) is insignificant for $\xi > \delta$. It is possible that this leads to a small amount of truncation error at high Reynolds numbers in the present problem. It is certainly more critical than in the flat plate problem for, although the wake is similar in both problems, only the frictional drag is present in the case of the flat plate and C_D varies as $R^{-\frac{1}{2}}$ as $R \to \infty$.

The variation of vorticity over the surface of the cylinder in the limiting solution as $R \to \infty$ is shown in figure 3. To some extent it is tentative since, as previously mentioned, it is not known precisely how the inclusion of further terms $g_n(\xi)$ in the series (11) would affect the estimation of the $G_n(0)$ in (46). It is, however, certain that it does not agree with Kawaguti's conjecture that as $R \to \infty$ the point of separation moves round the cylinder to the angle $\eta = 128.7^\circ$ given by Schmieden (1930) according to the discontinuous potential flow theory. This is impossible since, even at high Reynolds number, the terms involving $G_1(0)$ and $G_2(0)$ in (46) dominate the solution and they are of opposite sign so that ζ cannot vanish at an angle $\eta > 90^\circ$.

Finally, the pressure distribution over the surface of the cylinder is shown for various values of R in figure 16. It is obtained by integrating the appropriate equations of motion firstly along the axis $\eta = \pi$ from infinity to the surface of the cylinder, and then around the surface to the point with coordinate η. The result for the pressure p at station η on the surface is

$$\frac{p-p_\infty}{\frac{1}{2}\rho U^2} = 1 + \frac{4}{R}\int_0^\infty \left(\frac{\partial\zeta}{\partial\eta}\right)_\pi d\xi + \frac{4}{R}\int_\pi^\eta \left(\frac{\partial\zeta}{\partial\xi}\right)_0 d\eta \quad .$$

The trend of the distribution at R = 40 is similar to the calculations of Kawaguti and of Apelt, although the numerical values are somewhat different. The probable reason is that the present calculated value of the pressure drag at this value of R is higher than the result given by either of these authors. We cannot be sure of the reason for this, although it is possible that our result for the pressure drag is on the high side due to overestimation of the constant C_1.

REFERENCES

ALLEN, D.N. de G. and SOUTHWELL, R.V. 1955 Quart.J.Mech.Appl.Math.8,129.

APELT, C·J. 1961 Rep. and Memo., Aero.Res.Counc., Lond., No.3175.

BAIRSTOW, L.,CAVE, B.M. and LANG, E·D. 1923 Phil.Trans. A, 223, 383.

BLASIUS, H. 1913 Das Ähnlichtkeitsgesetz bei Reibungsvorgängen in Flüssigkeiten. Forschungsarbeiten d. VDI, Heft 131, S.177.

DENNIS, S.C.R. and DUNWOODY, J. 1964 The steady flow of a viscous fluid past a flat plate. To be published.

GOLDSTEIN, S· 1929 Proc.Roy.Soc. A, 123, 216.

GOLDSTEIN, S. 1938 Modern Developments in Fluid Dynamics, Vol.I, Ch.I. Oxford.

HOMANN, F. 1936 Forsch.Geb.Ing.Wes. 7, 1.

KAPLUN, S. 1959 J.Math.Mech. 6, 595.

KAWAGUTI, M. 1953 J.Phys.Soc.Japan, 8, 747.

KAWAGUTI, M. 1959 Quart.J.Mech.Appl.Math.12, 261.

LAMB, H. 1911 Phil.Mag.(6), 21, 112.

NISI, H. and PORTER, A.W. 1923 Phil.Mag.(6), 46, 754.

PROUDMAN, I, and PEARSON, J.R.A. 1957 J.Fluid.Mech.2, 237.

SCHMIEDEN, C. 1930 Ing.Arch.1, 104.

TANEDA, S. 1956 J.Phys.Soc.Japan, 11, 302.

THOM, A. 1930 Some studies of the flow past cylinders. Vorträge aus dem Gebiete der Aerodynamik und verwandter Gebiete by Gilles, Hopf and Karman (Aachen 1929), Berlin, p.58.

THOM, A. 1929 Rep. and Memo., Aero.Res.Counc., Lond., No.1194.

THOM, A. 1933 Proc.Roy.Soc. A, 141, 651.

TOMOTIKA, S. and AOI, T., 1950 Quart.J.Mech.Appl.Math.3, 140.

TRITTON, D.J. 1959 J.Fluid Mech.6, 547.

WATSON, G.N. 1944 Theory of Bessel functions. Cambridge.

WIESELSBERGER, C. 1921 Phys.Z. 22, 321.

R	Lamb	Kaplun	Dennis & Shimshoni
0.01	380.4	372.8	376.5
0.05	100.6	97.1	98.6
0.1	58.4	55.6	56.6
0.5	18.6	16.4	17.1

Table 1 : Comparison of C_D for low R

R	C_p	C_f	C_D	R	C_p	C_f	C_D
0.01	188.2	188.2	376.5	20	1.42	0.910	2.33
0.05	49.31	49.25	98.56	40	1.35	0.640	1.99
0.1	28.30	28.27	56.57	80	1.33	0.451	1.78
0.5	8.56	8.50	17.06	160	1.32	0.317	1.64
1	5.24	5.13	10.37	320	1.31	0.222	1.53
2	3.45	3.28	6.73	640	1.31	0.157	1.47
4	2.38	2.13	4.51	1280	1.31	0.112	1.42
7	1.88	1.56	3.44	10^4	1.30	0.043	1.34
10	1.69	1.30	2.99	10^5	1.30	0.014	1.31

Table 2 : Calculated drag coefficients

R	C_1	$G_1(0)$	$G_2(0)$	$G_3(0)$	$G_4(0)$	$G_5(0)$
0.01	-0.2996	1.000	-0.008	-	-	-
0.05	-0.3919	1.000	-0.029	-	-	-
0.1	-0.4501	1.000	-0.047	-	-	-
0.5	-0.6764	1.000	-0.149	-	-	-
1	-0.8165	1.000	-0.225	-	-	-
2	-1.045	1.000	-0.322	0.001	-0.001	-
4	-1.356	1.000	-0.442	0.005	-0.002	-0.001
7	-1.734	1.000	-0.560	0.010	-0.003	-0.002
10	-2.070	1.000	-0.619	0.015	-0.003	-0.003
20	-2.912	1.000	-0.719	0.035	-0.023	-0.013
40	-4.077	1.000	-0.847	0.054	-0.028	-0.023
80	-5.737	1.000	-0.964	0.063	-0.045	-0.031
160	-8.073	1.000	-1.036	0.068	-0.054	-0.036

Table 3 : Vorticity on cylinder surface

D 31170/1/Wt.60 K4 3/65 XL & CL

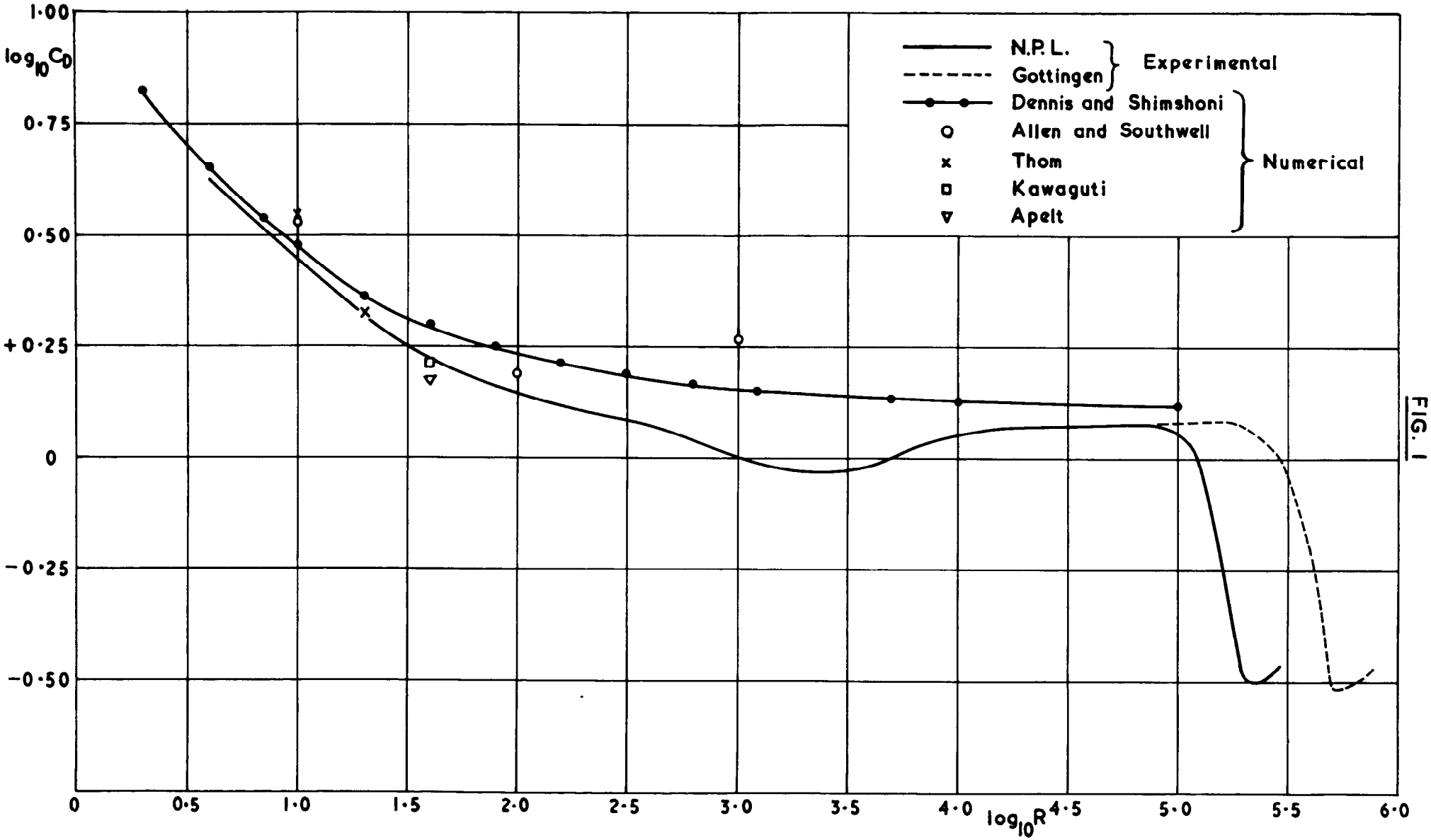
1·00
$\log_{10} C_D$
0·75
0·50
+0·25
0
−0·25
−0·50
0
0·5
1·0
1·5
2·0
2·5
3·0
3·5
4·0
4·5
5·0
5·5
6·0
$\log_{10} R$
N.P.L.
Gottingen
Experimental
Dennis and Shimshoni
Allen and Southwell
Thom
Kawaguti
Apelt
Numerical

FIG. 1

FIG. 2

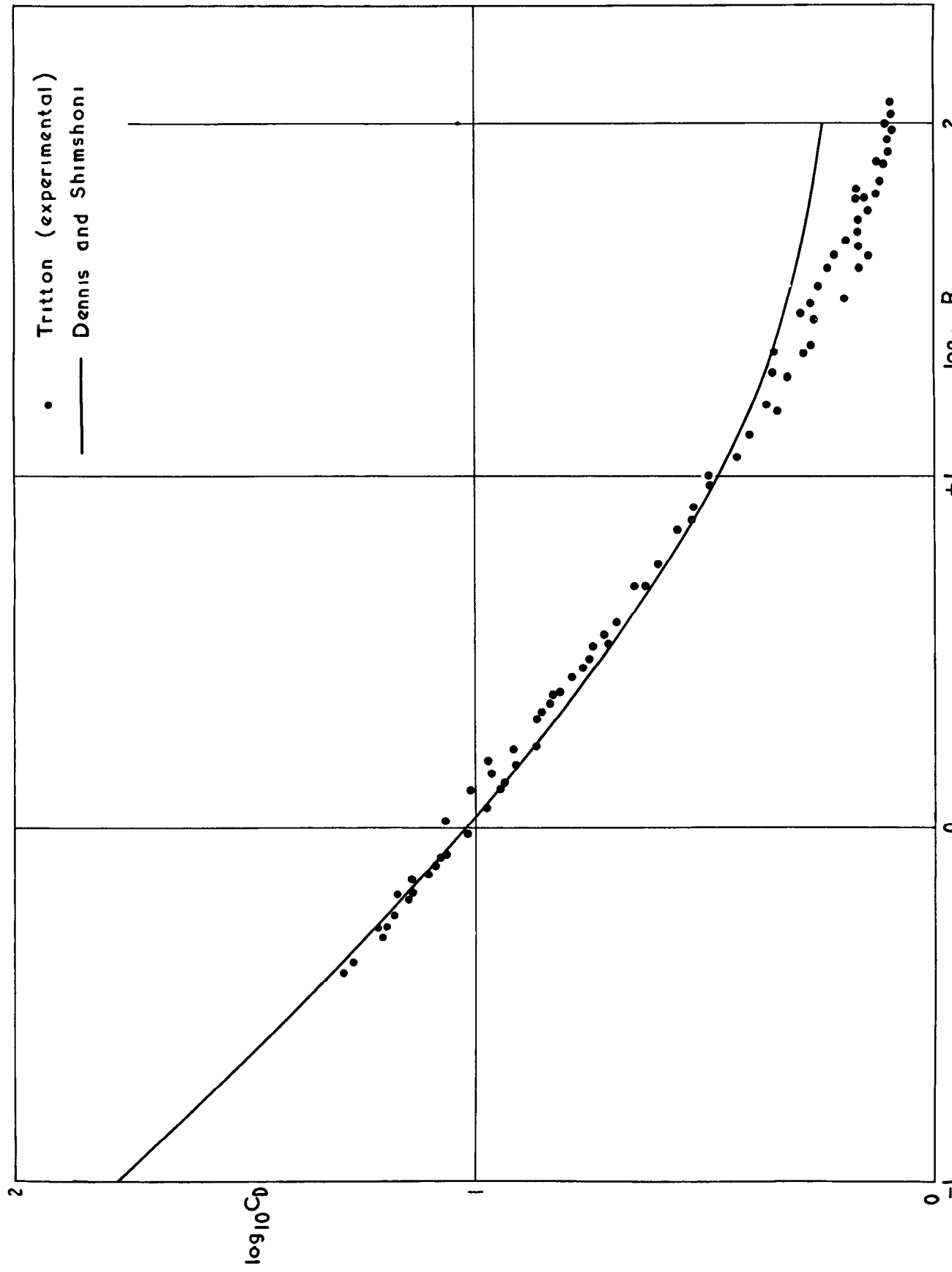
Tritton (experimental)
Dennis and Shimshoni
$\log_{10} C_D$
$\log_{10} R$
2
1
0
−1
0
+1
2

FIG 3

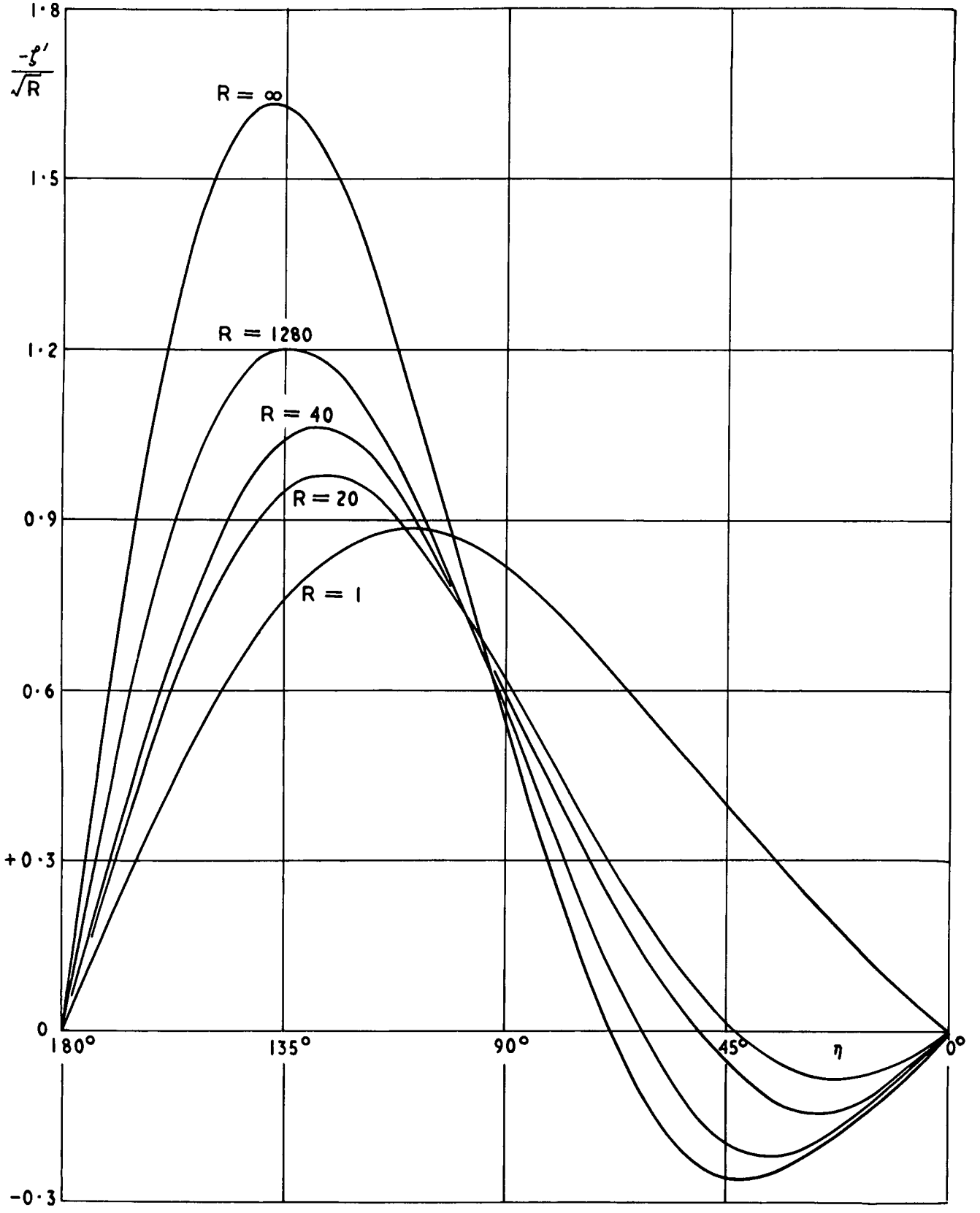

(ζ' = dimensionless scalar vorticity)

FIG. 4

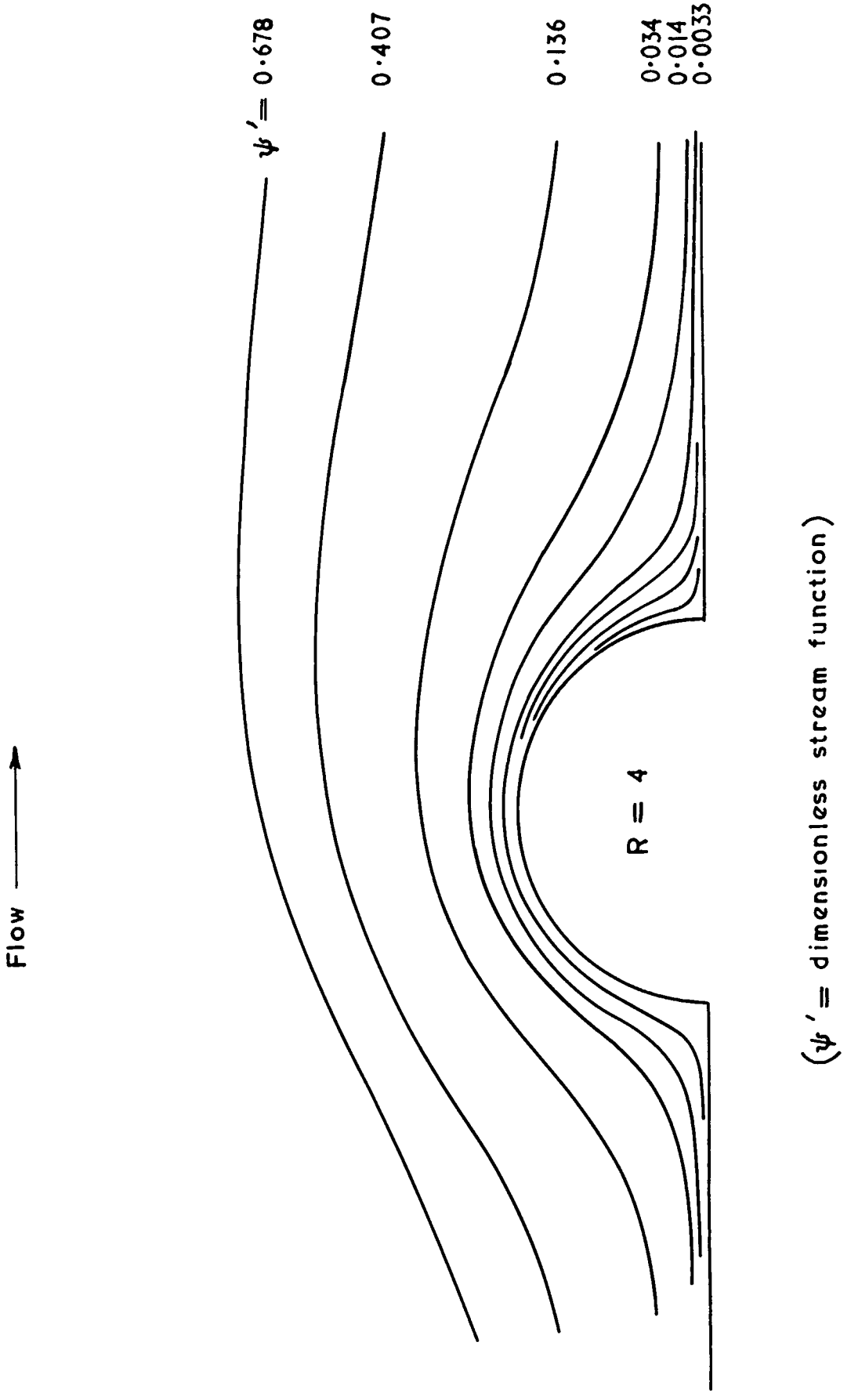

(ψ' = dimensionless stream function)

FIG. 5

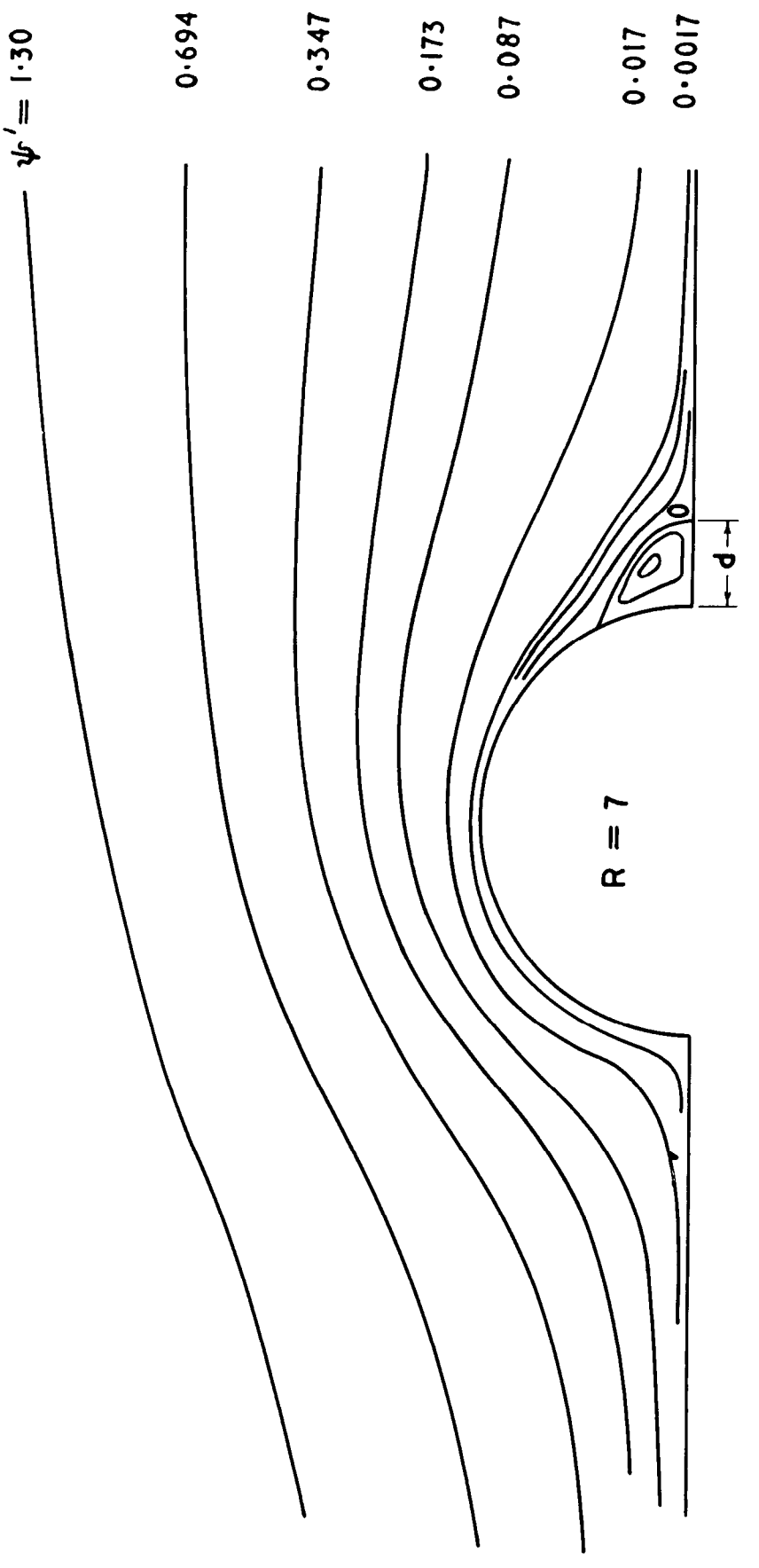

FIG. 6

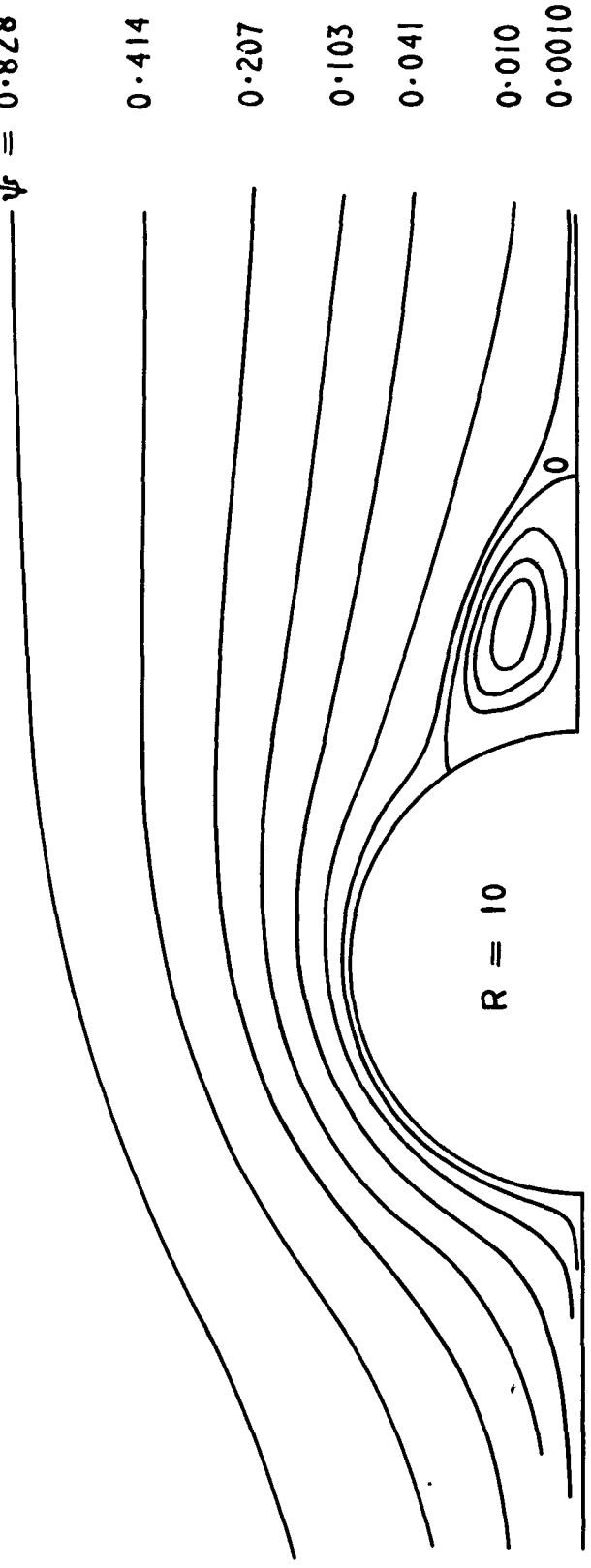

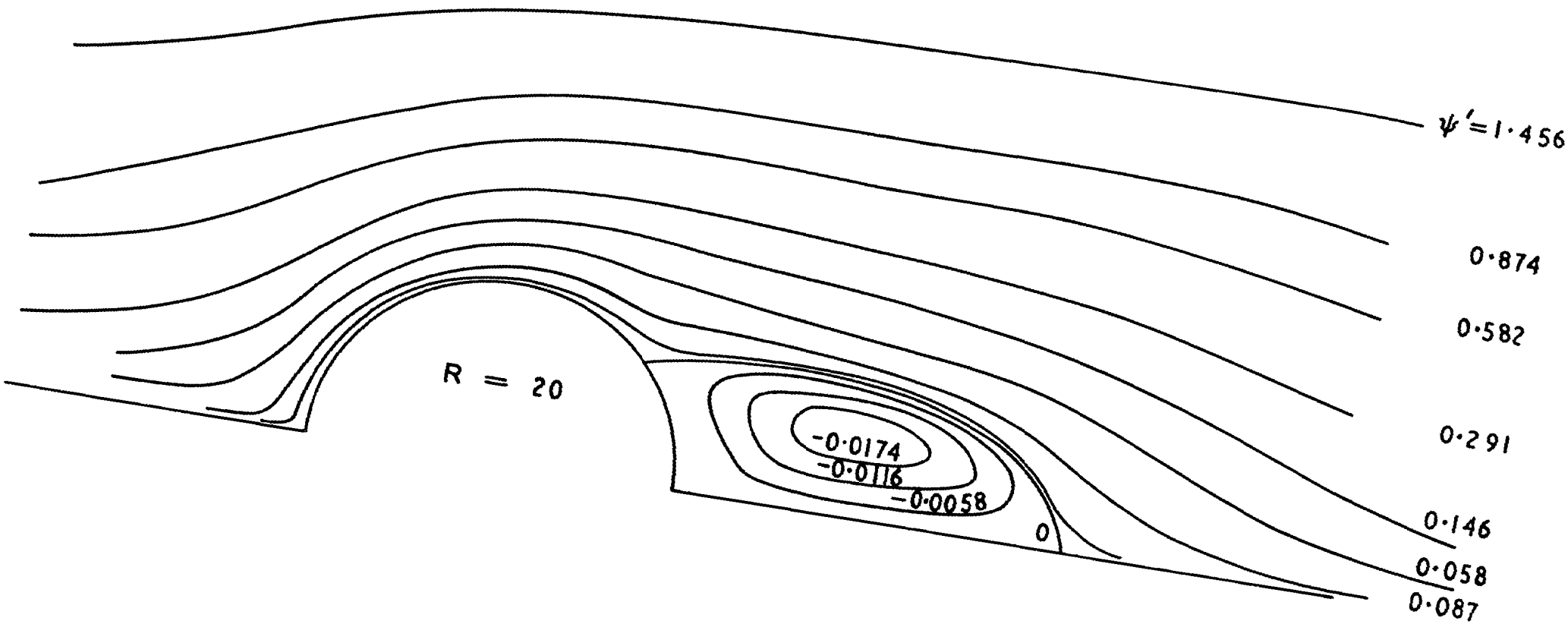
$\psi' = 1 \cdot 456$
0·874
0·582
0·291
0·146
0·058
0·087
R = 20
-0·0174
-0·0116
-0·0058
0

FIG. 7

FIG. 8

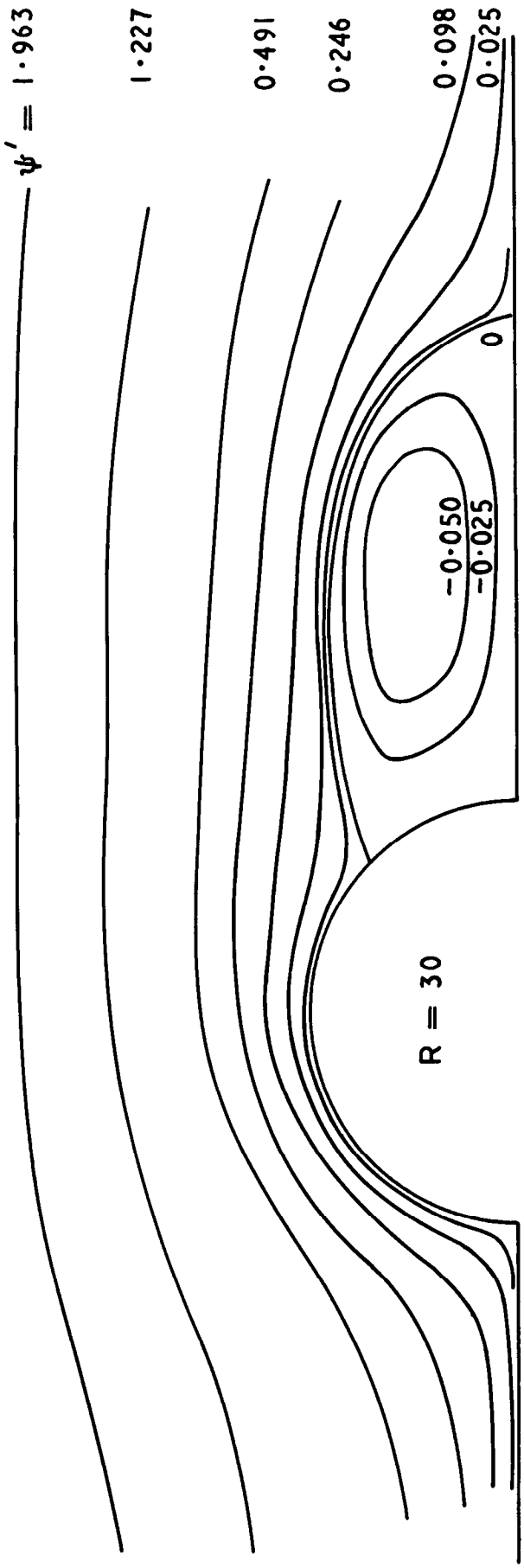

FIG. 9

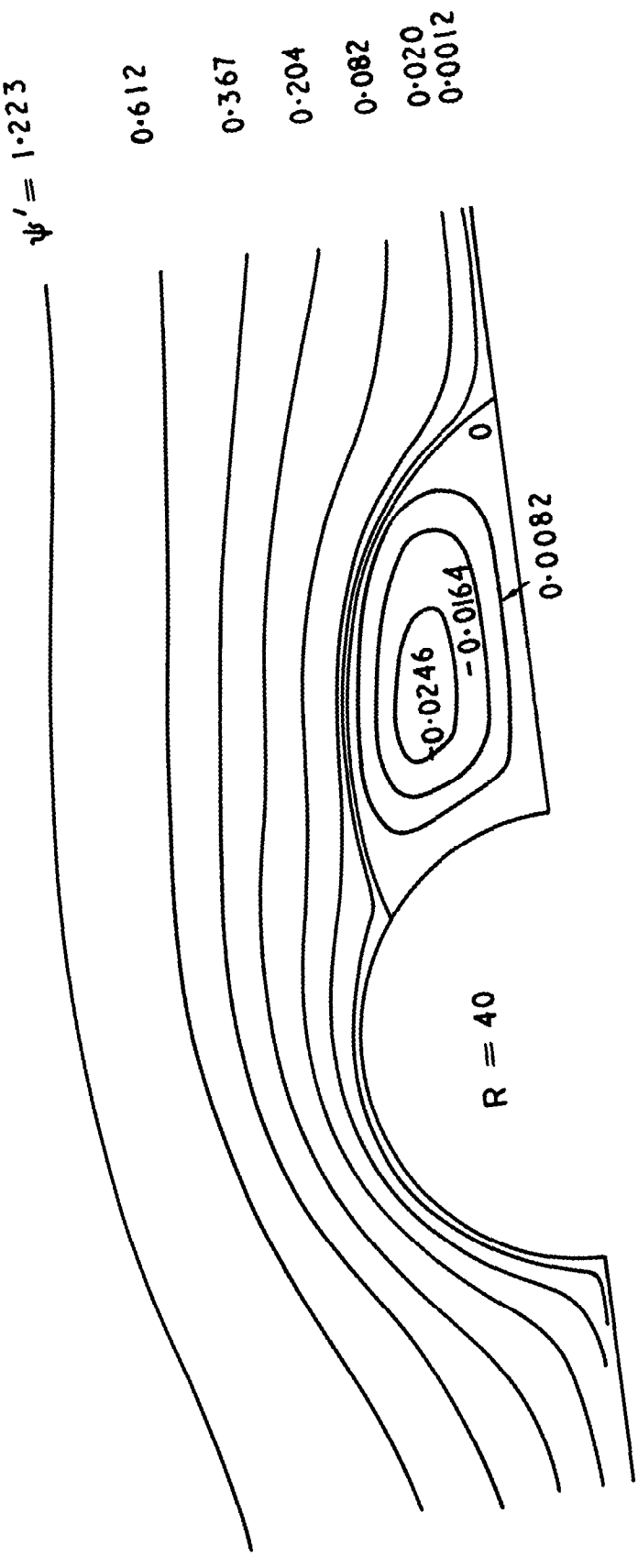

FIG. 10

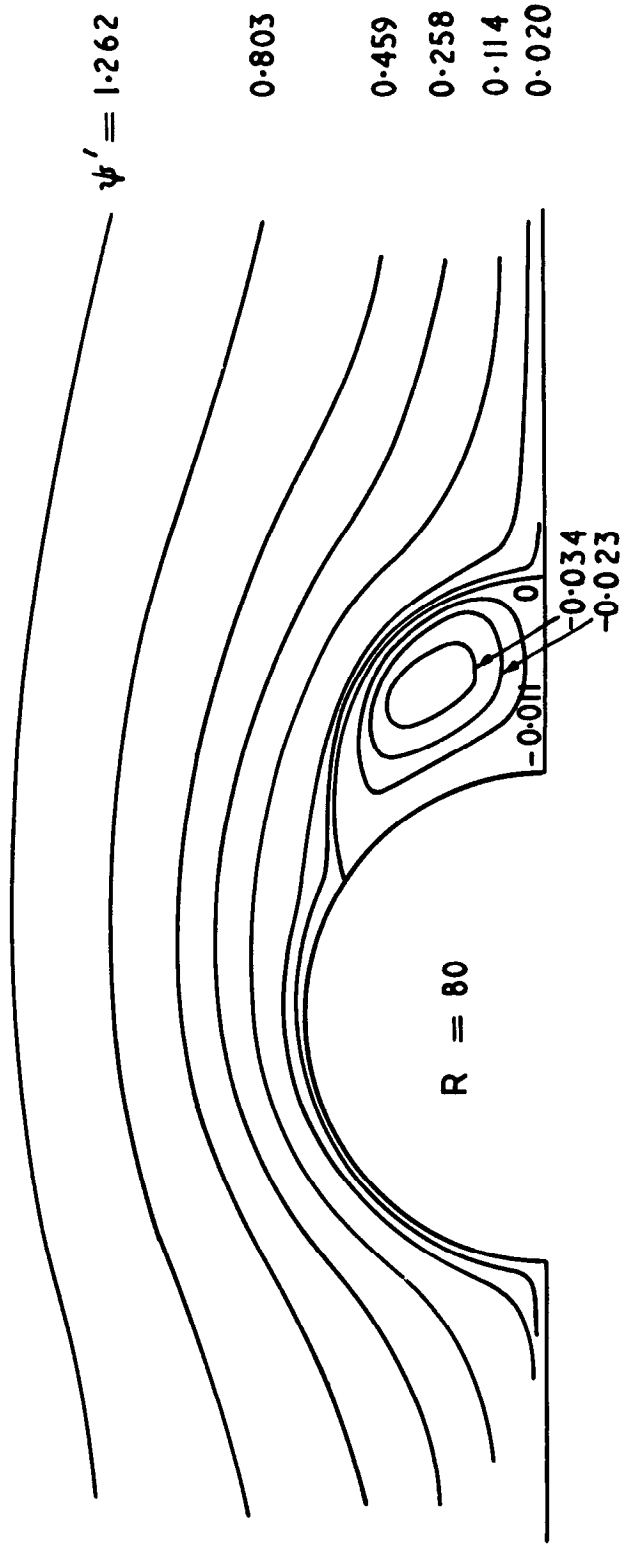

FIG. 11

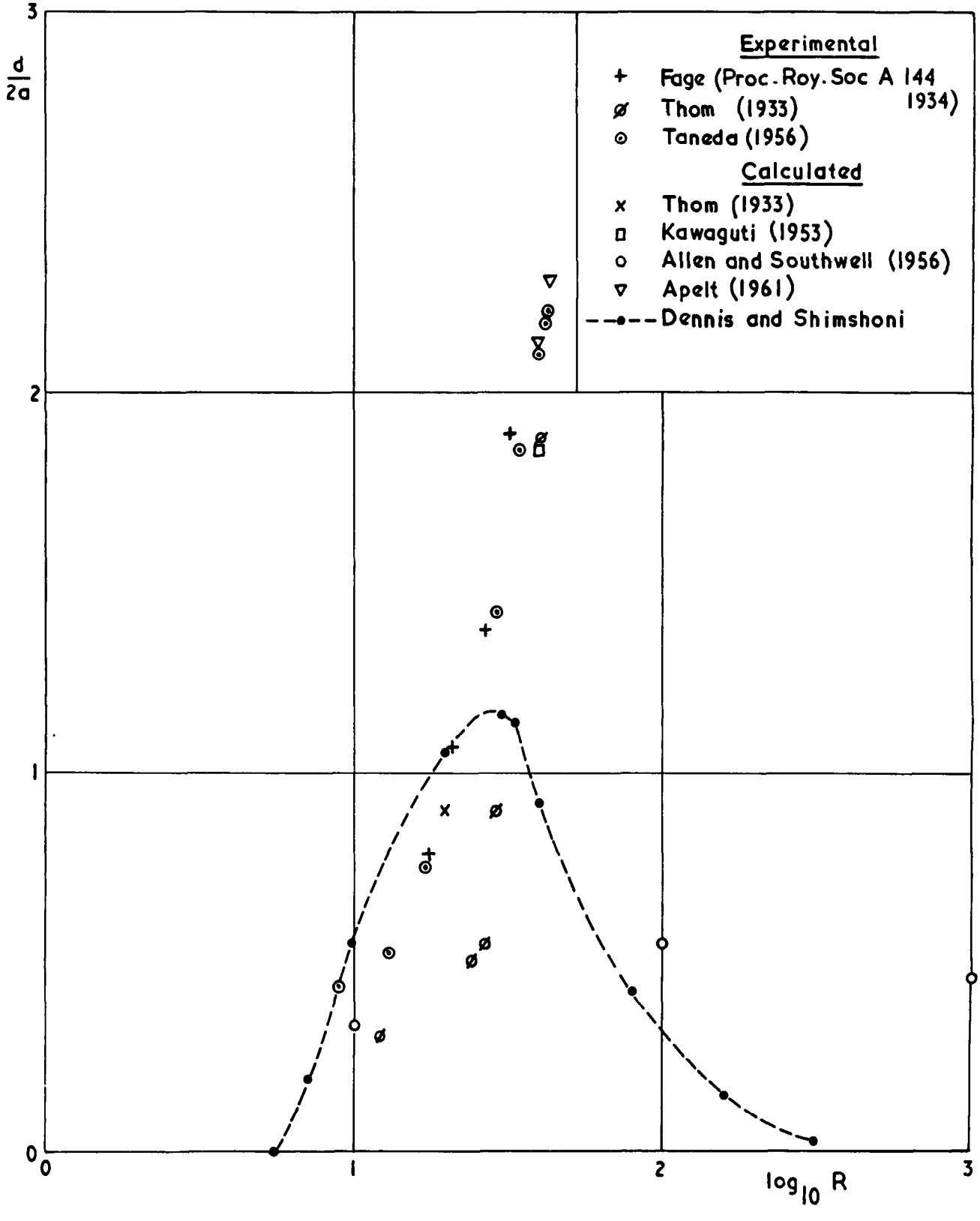
Experimental
Fage (Proc. Roy. Soc A 144 1934)
Thom (1933)
Taneda (1956)
Calculated
Thom (1933)
Kawaguti (1953)
Allen and Southwell (1956)
Apelt (1961)
Dennis and Shimshoni
d/2a
log10 R
0
1
2
3

FIG. 12

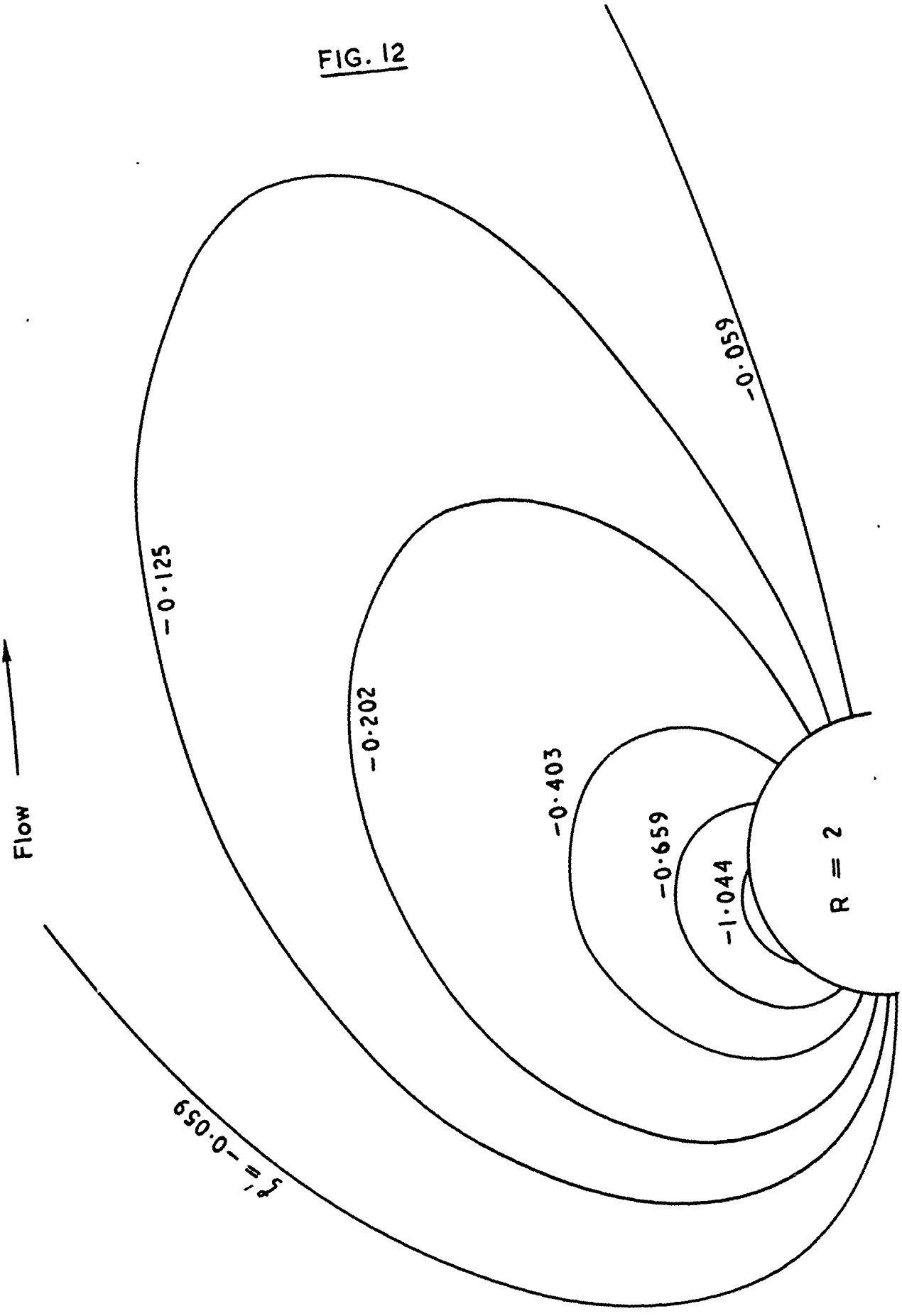

FIG. 13

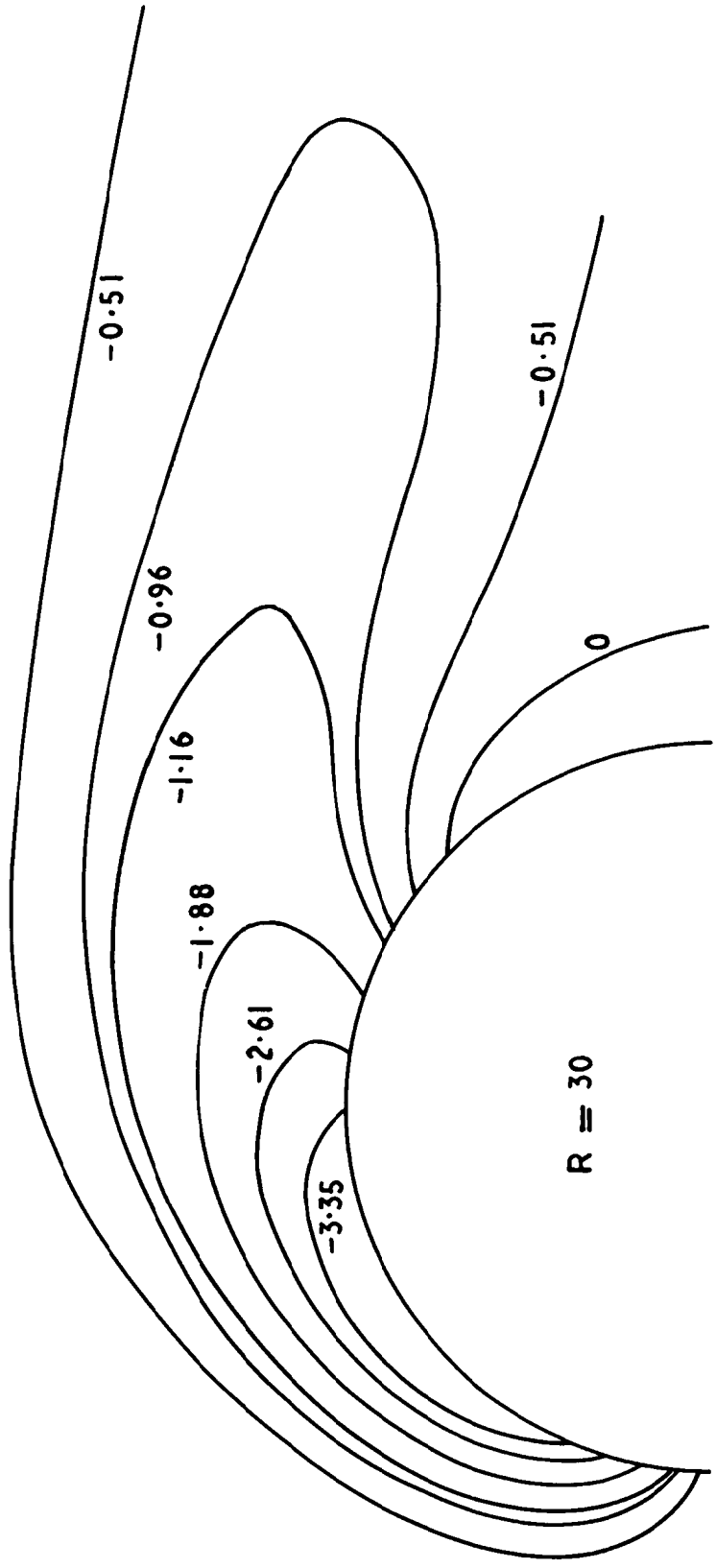

FIG. 14

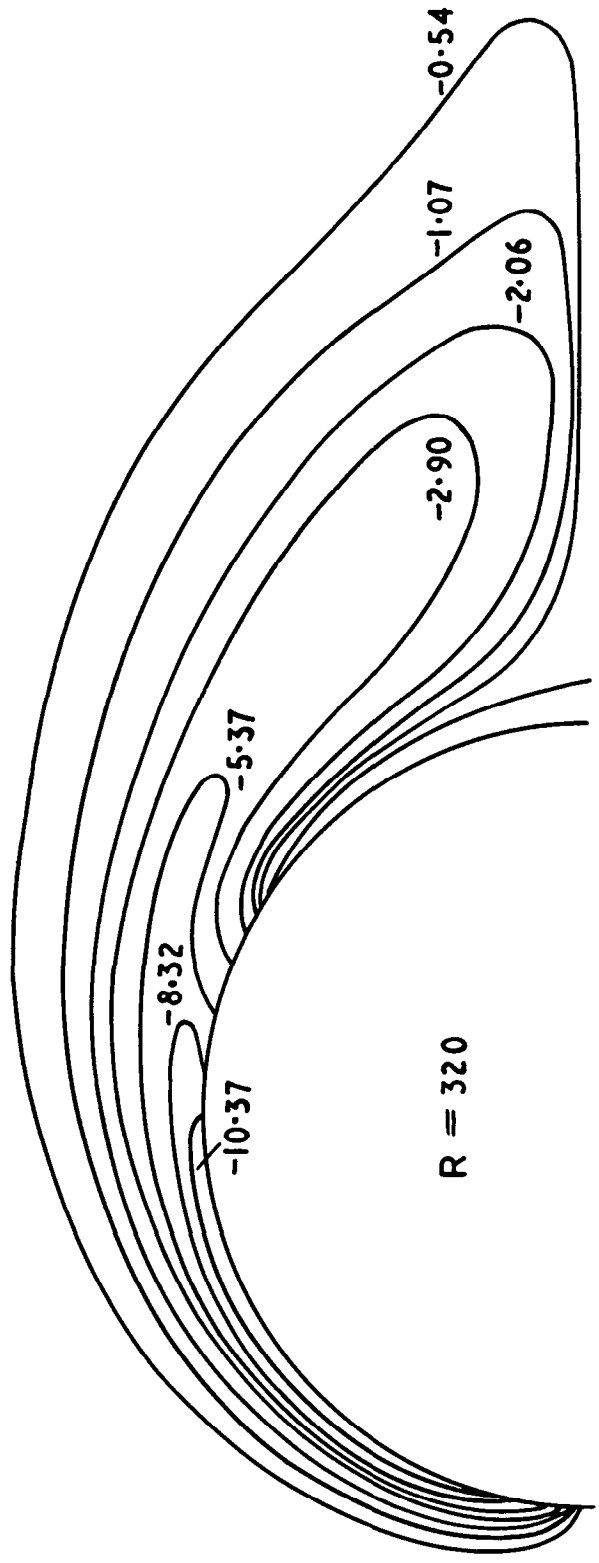

FIG. 15

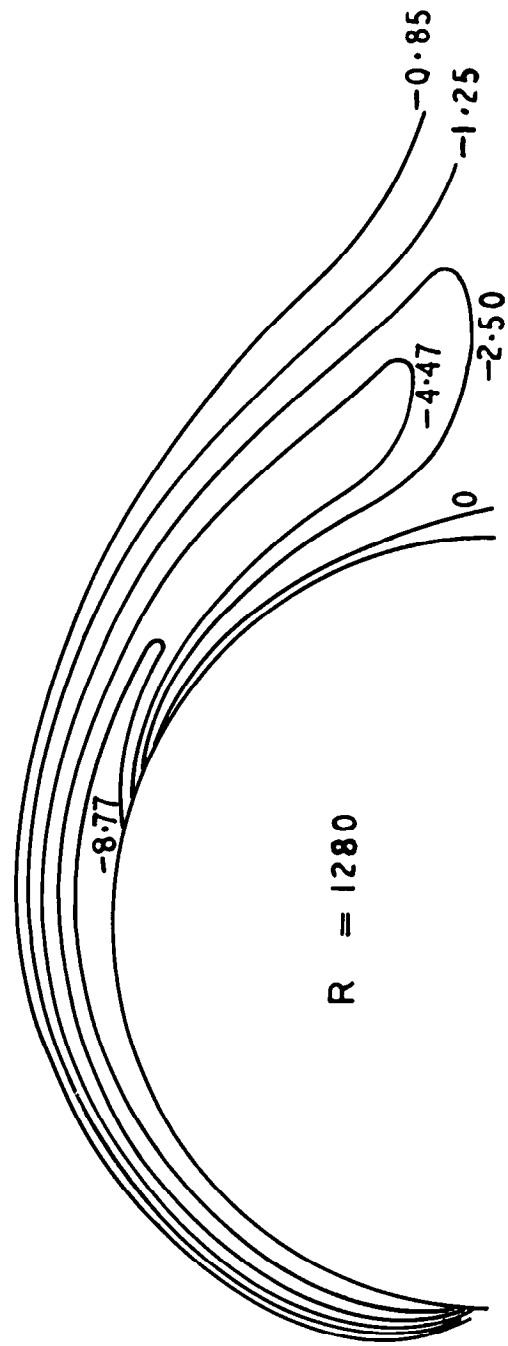

FIG. 16

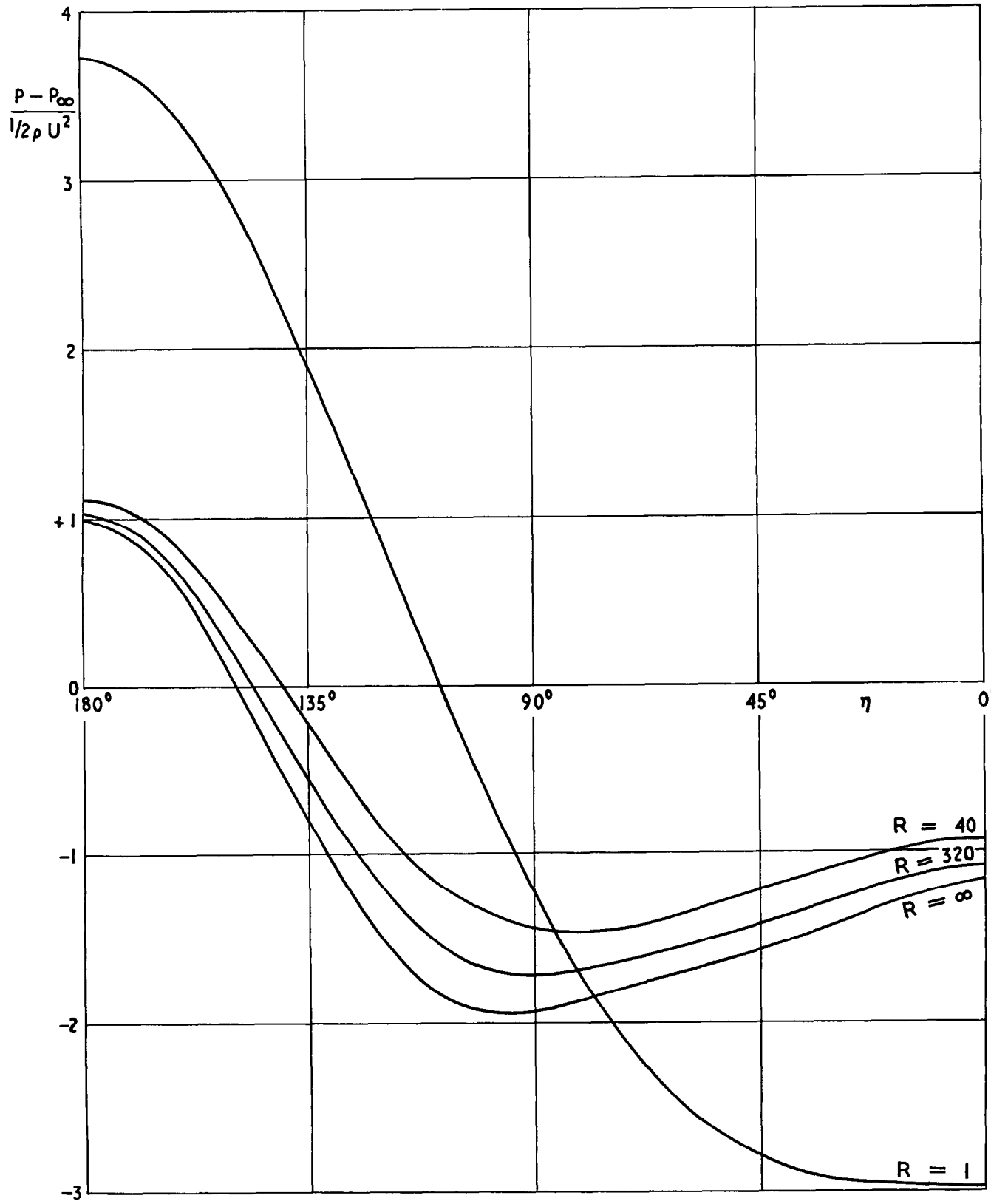

A.R.C. C.P. No. 797
August, 1961.
S. C. R. Dennis (University of Sheffield) and
M. Shimshoni (Weizmann Institute, Rehovot, Israel).

THE STEADY FLOW OF A VISCOUS FLUID PAST A CIRCULAR CYLINDER

Using numerical methods described by Dennis and Dunwoody, the steady motion of a viscous, incompressible fluid past a fixed circular cylinder is investigated over the complete range of Reynolds numbers. In particular, the limiting solution as the Reynolds number R becomes large is considered.

The calculated drag coefficient is found to agree reasonably well with experimental measurements for low Reynolds numbers but starts to become higher for values of R greater than 30.

The calculations show that a standing vortex pair, behind the cylinder, first appears at R = 5·6 which is in good agreement with the experimental results of Homann and Taneda.

A.R.C. C.P. No. 797
August, 1964.
S. C. R. Dennis (University of Sheffield) and
M. Shimshoni (Weizmann Institute, Rehovot, Israel).

THE STEADY FLOW OF A VISCOUS FLUID PAST A CIRCULAR CYLINDER

Using numerical methods described by Dennis and Dunwoody, the steady motion of a viscous, incompressible fluid past a fixed circular cylinder is investigated over the complete range of Reynolds numbers. In particular, the limiting solution as the Reynolds number R becomes large is considered.

The calculated drag coefficient is found to agree reasonably well with experimental measurements for low Reynolds numbers but starts to become higher for values of R greater than 30.

The calculations show that a standing vortex pair, behind the cylinder, first appears at R = 5·6 which is in good agreement with the experimental results of Homann and Taneda.

A.R.C. C.P. No. 797
August, 1964.
S. C. R. Dennis (University of Sheffield) and
M. Shimshoni (Weizmann Institute, Rehovot, Israel).

THE STEADY FLOW OF A VISCOUS FLUID PAST A CIRCULAR CYLINDER

Using numerical methods described by Dennis and Dunwoody, the steady motion of a viscous, incompressible fluid past a fixed circular cylinder is investigated over the complete range of Reynolds numbers. In particular, the limiting solution as the Reynolds number R becomes large is considered.

The calculated drag coefficient is found to agree reasonably well with experimental measurements for low Reynolds numbers but starts to become higher for values of R greater than 30.

The calculations show that a standing vortex pair, behind the cylinder, first appears at R = 5·6 which is in good agreement with the experimental results of Homann and Taneda.

Printed and published by
HER MAJESTY'S STATIONERY OFFICE

To be purchased from
York House, Kingsway, London w c 2
423 Oxford Street, London w 1
13A Castle Street, Edinburgh 2
109 St Mary Street, Cardiff
39 King Street, Manchester 2
50 Fairfax Street, Bristol 1
35 Smallbrook, Ringway, Birmingham 5
80 Chichester Street, Belfast 1
or through any bookseller

Printed in England

S.O. Code No. 23-9015-97